Article AR2482 DOI: HTTPS://DOI.ORG/10.23910/1.2021.2482

International Journal of Bio-resource and Stress Management

December 2021

Crossref

Print ISSN 0976-3988

Online ISSN 0976-4038

IJBSM 2021, 12(6):745-750

Research Article *Natural Resource Management*

Monitoring of Spectral Signatures of Maize Crop using Temporal SAR and Optical Remote Sensing data

D. Anil Kumar[1], P. Srikanth[2], T. L. Neelima[1*], M. Uma Devi[1], K. Suresh[3] and C. S. Murthy[1]

[1]Water Technology Centre, [3]Examination centre, Professor Jayashankar Telangana State Agricultural University, Rajendranagar, Hyderabad, Telengana (500 030), India

[2]Agricultural Sciences and Applications Group, Remote Sensing-Applications Area, National Remote Sensing Centre, Indian Space Research Organization, Hyderabad, Telengana (500 037), India

Corresponding Author

T. L. Neelima

e-mail: neelimalakshmi@gmail.com

Citation: Kumar et al., 2021. Monitoring of Spectral Signatures of Maize Crop using Temporal SAR and Optical Remote Sensing data. International Journal of Bio-resource and Stress Management 2021, 12(6), 745-750. HTTPS://DOI.ORG/10.23910/1.2021.2482.

Data Availability Statement: Legal restrictions are imposed on the public sharing of raw data. However, authors have full right to transfer or share the data in raw form upon request subject to either meeting the conditions of the original consents and the original research study. Further, access of data needs to meet whether the user complies with the ethical and legal obligations as data controllers to allow for secondary use of the data outside of the original study.

Conflict of interests: The authors have declared that no conflict of interest exists.

Acknowledgement: The authors immensely thank National Remote Sensing Centre, Hyderabad, India for providing the technical guidance and assisting the student in carrying out this work.

Abstract

A study was carried out using the temporal Sentinel-1B microwave data (June to November at 12 days interval) and Sentinel-2A/2B optical data (June to November) to discriminate the maize crop from other competing crops rice and cotton in Siddipet district, Telangana state, India during *kharif*, 2019 (June to November). The study utilized the data from multiple sources such as Multi-temporal VH backscatter intensity from Sentinel-1B SAR and NDVI values from Sentinel-2A/2B in combination with field data to discriminate the maize crop. Synchronous to satellite pass, ground truth data on crop parameters *viz.,* crop stage, crop vigour, biomass, plant height, plant density, soil moisture, LAI and chlorophyll content were collected. Multi-temporal VH backscatter intensity and Normalized Difference Vegetation Index (NDVI) data were used to characterize backscatter and greenness behaviour of the maize crop. The backscatter intensity (dB) for maize crop ranged from -21.83 (the lowest backscatter values) at planting to -12.52 (the highest backscatter values) at peak growth stage. The NDVI values during vegetative and reproductive stages (August and September) were >0.6 and during senescence to harvesting the values were less than or equal to 0.52. The increase in backscatter intensity values from initial vegetative stage to peak stage was due to increased volume scattering of the maize crop canopy and a continuous decline in backscatter intensity values of VH band at maturity stage, was due to decrease in greenness and moisture content in leaves of the maize crop helped in maize crop discrimination from other dominant *kharif* crops in the study area.

Keywords: Maize, remote sensing, sentinel, spectral signature, VH backscatter

1. Introduction

The maize crop is grown throughout the year in India. However, 85% of it's area is under cultivation during *kharif* season (Anonymous, 2019). India contributes 2.5% of the world maize production. Globally, maize is globally a top ranked cereal, not only in productivity but also as staple food for human beings, quality feed for animals, maize serves as a basic raw material as an ingredient to innumerable number thousands of industrial products which includes starch, oil, protein, alcoholic beverages, food sweeteners, pharmaceutical, cosmetic, film, textile, gum, package and paper industries etc., (Murdia et al., 2016). There is a unique challenge for the researchers to meet the needs of future generation for

Article History

RECEIVED on 02nd July 2021 RECEIVED in revised form on 02nd November 2021 ACCEPTED in final form on 23rd December 2021

new products derived from maize. Major proportion (55%) of maize is consumed as food and also utilized as feed, forage and in processing industry. Nevertheless, maize is now gaining importance on account of its potential uses in manufacturing of starch, resins, syrups, ethanol *etc*., (Kumar and Jharia, 2013; Singh et al., 2021). Therefore, a reliable maize crop map is a key input parameter for the decision makers for planning purposes and policy making related to its production.

Crop discrimination is a critical step for most agricultural monitoring systems (Dave et al., 2019). Acquiring annual crop information using traditional survey methods are very difficult due to less economic efficiency, larger area, strong seasonal and spatial heterogeneity. The use of remote sensing technology is the more effective way to solve this issue (Changan et al., 2019). Optical remote sensing for crop monitoring has increased over the past several years and become one of the major civilian operational applications. Since different crop types may have similar reflectance properties in visible regions, the use of remote sensing technology to differentiate crops is a demanding task (Waldhoff et al., 2012; Zhou et al., 2017; Gali et al., 2020; Snehalatha et al., 2021). Crops having similar reflectance properties can only be separated from each other by multi-temporal analysis.

Optical images are not always available at phenological stages for crop discrimination due to cloud and haze interference and the when there is a gap in data acquisition during critical growth periods, classification accuracies using optical data are often inadequate (McNairn et al., 2002; Blaes et al., 2005; Ram et al., 2014). The mid to late season optical images are generally used to achieve crop classification and this dependency on late-season data reduces the ability to deliver early season crop acreage estimates (Shang et al., 2006; McNairn et al., 2009). These constraints seriously impede the use of optical data for monitoring *kharif* season crops.

Due to the greater wavelength compared to visible and infrared radiation, microwaves exhibit the important property of penetration through clouds, fog and possible ash or powder coverages. This important property makes this technique virtually suitable to work in any weather condition or environment. Crop growth cycle in a season could be monitored based on the changes in SAR backscattering in response to phenological stages of a particular crop. Analysis of multi-temporal C-band and L-band, airborne and space-borne SAR data showed that the relations between the backscattering of crops and the vegetation biomass depend on plant type, and that there are different trends for “narrow” and “broad” leaf crops (Macelloni et al.,2001).

In this study, potential of time-series Sentinel-1 backscatter data in combination with Sentinel-2 reflected data for the maize crop discrimination is explored. Multi-temporal C-band VH polarized Sentinel-1 SAR data was evaluated for the backscatter behavior of maize crop and monthly interval stack NDVI values from Sentinel-2 optical data to fine-tune maize crop map in Siddipet district, Telangana state.

2. Materials and Methods

2.1. Study area

The study area is located in Siddipet district which agro-climatologically comes under the Central Telangana Zone, with 18.12°N Latitude and 78.85°E Longitude (Figure 1). The study was taken up during *kharif*, 2019 (June to November). It is one of the major districts in area and production of maize crop in Telangana state. The climate in the district is tropical and is characterized by hot summer and dry conditions except during the south-west monsoon season. The mean daily maximum and minimum temperature is 41°C and 27°C and during summer, the days are intensively very hot and the temperature may rise up to 44°C. The average annual rainfall of the district is 812 mm. The major soil type in Siddipet district is Alfisol and to a little extent Vertisol. Rice, maize and cotton during *kharif* season and bengalgram, sunflower and chillies during *rabi* season are the predominant crops grown in the district.

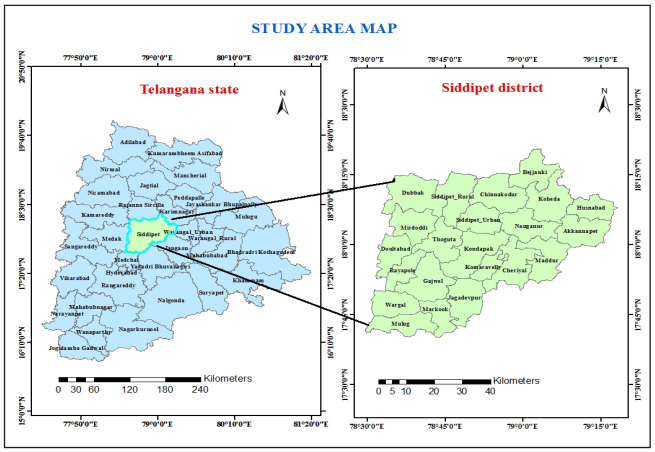

Figure 1: Study area location of Siddipet district in Telangana state

2.2. Data used

2.2.1. Sentinel-1 SAR data

The time series dual-polarized (VV/VH) C-band imagery of Sentinel-1B operating at a radar wavelength of about 5.6 cm, with a repeat cycle of 12 days from the European Space Agency (ESA), covering 2019 maize crop growing season was used for the study. In this study, level-1 ground range detected product, which provides multi-looked backscatter intensity normalized with respect to area in VH and VV polarizations, with a swath width of approximately 250 km and a spatial resolution of 10 m was used. A total of 15 scenes with a descending orbit during June to November 2019 were used in the analysis. The details of the Sentinel-1B data acquisition dates are given in Table 1.

2.2.2. Sentinel-2 MSI data

Sentinel-2 mission is a constellation with two satellites

Table 1: Sentinel-1B acquisition dates and other specifications

Sl. No.	Date of pass	Scene number	Pass direction	Orbit number
1.	11-06-2019	80AB	Descending	16641
2.	11-06-2019	6B34	Descending	16641
3.	23-06-2019	E189	Descending	16816
4.	23-06-2019	A974	Descending	16816
5.	05-07-2019	DD50	Descending	16991
6.	05-07-2019	D3DC	Descending	16991
7.	17-07-2019	2239	Descending	17166
8.	17-07-2019	7B7F	Descending	17166
9.	29-07-2019	7B6A	Descending	17341
10.	29-07-2019	9C66	Descending	17341
11.	10-08-2019	9F3B	Descending	17516
12.	22-08-2019	D5FD	Descending	17691
13.	03-09-2019	COO2	Descending	17866
14.	03-09-2019	4D31	Descending	17866
15.	15-09-2019	4071	Descending	18041
16.	15-09-2019	6CCD	Descending	18041
17.	27-09-2019	BC9A	Descending	18214
18.	27-09-2019	D9F2	Descending	18214
19.	09-10-2019	3F5E	Descending	18391
20.	09-10-2019	4E4E	Descending	18391
21.	21-10-2019	8A51	Descending	18566
22.	21-10-2019	A4F6	Descending	18566
23.	02-11-2019	0E1E	Descending	18741
24.	02-11-2019	0E1E	Descending	18741
25.	14-11-2019	9189	Descending	18916
26.	14-11-2019	30B7	Descending	18916
27.	26-11-2019	5FC1	Descending	19091
28.	26-11-2019	A8CF	Descending	19091

(Sentinel-2A and 2B) by ESA with a multi-spectral sensor (MSI) with thirteen spectral channels in the visible/near infrared (VNIR) and short-wave infrared spectral range (SWIR) at spatial resolutions of 10 m, 20 m and 60 m, respectively. Both sentinel-2A and 2B satellite data collected during crop growth period at a monthly interval from June to November month (1 FN June, July, August, September, October, 1 FN November). The MSI bands of Blue (B2), Green (B3), Red (B4) and NIR (B8) were used prepare false colour composite (FCC) of 10m spectral resolution. NDVI images were developed from FCC and were layer stacked to create one single NDVI stack image.

All images from Sentinel satellite constellations are freely available and can be downloaded at https://scihub.copernicus.eu/dhus/#/home.

2.2.3. Ground reference data

Field information on the *kharif* crops in the maize growing districts of Siddipet district were collected using FASAL app, a mobile application developed by NRSC during *kharif*, 2019. The information on various parameters like crop type, sowing, moisture content in the soil, planting geometry, crop stage and the probable date of harvest, were collected during the field visit, using mobile app. This aided in efficient collection of ground information about the crop along with field photographs.

2.3. Methodology

Temporal Sentinel-1 and Sentinel-2 data were used to discriminate maize crop and the methodology is explained in detail.

2.3.1. Data pre-processing

Sentinel-1B SAR pre-processing includes radiometric calibration, speckle filtering, geometric calibration carried out in SNAP software version 7.0 Desktop (Sentinel application platform. The ERDAS imagine 2018 was used for image analysis, classification etc., and Arc GIS was used for map composition.

2.3.2. Radiometric calibration

The objective of SAR calibration is to provide imagery in which the pixel values can be directly related to the radar backscatter of the scene. Though uncalibrated SAR imagery is sufficient for qualitative use, calibrated SAR images are essential to quantitative use of SAR data. Typical SAR data processing, which produces level 1 images, does not include radiometric corrections and significant radiometric bias remains. Therefore, it is necessary to apply radiometric correction to SAR images so that the pixel values of the SAR images truly represent the back scatter of the reflecting surface. The radiometric correction is also necessary for the comparison of SAR images acquired with different sensors or acquired from the same sensor but at different time, in different modes, or processed by different processors.

2.3.3. Speckle filter operator

SAR images have texturing like appearance called speckles which degrade the quality of the image and make interpretation of features more difficult. Speckles are caused by random constructive and destructive interference of the de-phased but coherent return waves scattered by the elementary scatters within each resolution cell. Speckle noise reduction can be applied either by spatial filtering or multilook processing.

2.3.4. Range doppler terrain correction operator

Due to topographical variations of a scene and tilt of the satellite sensor, distances can be distorted in the SAR images. Image data which is not directly at the sensor's Nadir location will have some distortion. Terrain corrections are intended to compensate for these distortions so that the geometric representation of the image will be as done as possible to real world.

2.3.5. Extraction of spectral signatures

These multi-temporal VH backscatter images were layer stacked and are used in Spectral profiles monitoring. Similarly, Sentinel-2 MSI data were converted in to NDVI images and then layer stacked for extraction of NDVI statistics. Backscatter (dB) values of VH-polarization were extracted from the temporal backscatter intensity image (15 layers) and the mean NDVI values were extracted from the monthly/fortnightly NDVI maximum value composite images (6 layers) using field points. Further, VH backscatter and NDVI values were used to generate temporal profiles of maize and cotton crops. The detail procedure for Spectral profile analysis is shown in Figure 2. These spectral profiles were analyzed for identifying the sowing period, maximum vegetation period and maturity period of maize crop. Maize crop sowings start from 2nd fortnight of June to 1st fortnight of July and peak growth was observed during October and harvestings will be completed during 2nd fortnight of October to 1st fortnight of November.

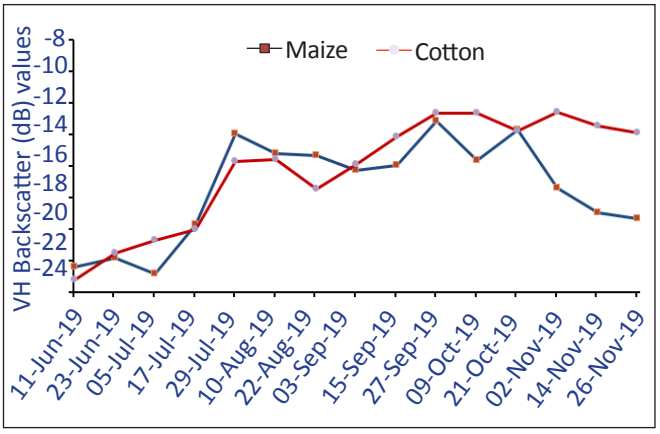

Figure 2: Temporal VH backscatter profiles of maize and cotton crops grown in Siddipet district

3. Results and Discussion

The spectral signatures and its temporal variations of different crops were analysed based on training data sets of study area. Spectral signature of different crops were extracted from the temporal images of VH and NDVI images. The training sets (AOI) were overlaid on the study area image and the mean back scatter values (dB) of each training site was extracted. The resulted back scattered values were analysed for sowing time, peak growth stage and maturity/ harvesting stage of crops during *kharif* season.

The characterization of maize crop was carried out based on two main assumptions: (i) the growth rate of maize crop is higher than cotton crop during initial phase and this led to increase in the backscatter values in VH polarization than cotton and (ii) Maize entered the senescence phase earlier to cotton crop. Maize crop phenological information were analyzed using the temporal VH backscatter data and temporal NDVI data. The ground truth information collected on sowing time, onset of peak growth stage, senescence stage and length of growing period was used to support the discrimination of maize crop.

3.1. Temporal behavior of maize from Sentinel-1 SAR and Sentinel-2 NDVI data

Maize crop showed significant temporal behavior and greater dynamic range in the crop-cultivated regions of the study area during the crop growth period. Temporal backscatter values were recorded for maize crop in test sites across Siddipet district and the details are presented in Table 2 and illustrated in Figure 2. An increase in the backscattering coefficient from -22.38 to -22.17 and -15.14 to -13.98 dB for first five acquisitions (11th June, 23rd June, 5th July, 17th July and 29th July) during the crop growth period that was typical of seedling to peak vegetative stage and a slight decrease from peak vegetative growth to tasseling phase (-15.21 to -13.96 and -16.28 to -15.13 dB) during the later period acquisitions (10th Aug, 22nd Aug, 3rd Sep). There was marginal increase in backscattering coefficients (-15.98 to -15.50 and -13.70 to -12.52 dB) at later reproductive stages (15th Sep, 27th Sep, 9th Oct and 21st Oct) and there after continuous decline in backscatter intensity of VH band values from -17.37 to -19.34 dB at maturity stages (2nd Nov, 14th Nov and 26th Nov). Similarly, the backscattering coefficient for cotton crop showed increasing trend from -21.54 to -23.22 and -13.24 to -13.45 dB from 11th June to 14th Nov 2019 indicating the crop progression from emergence to pod formation stage.

Table 2: Backscatter intensity values of Temporal VH band (15 layers) for maize and cotton crops

Acquisition dates	Back scattering coefficients			
	Maize		Cotton	
11-Jun-19	-22.38	-22.17	-21.54	-23.22
23-Jun-19	-21.83	-20.37	-22.13	-21.48
5-Jul-19	-22.82	-21.59	-23.42	-20.72
17-Jul-19	-19.72	-21.77	-22.81	-20.01
29-Jul-19	-13.98	-15.14	-15.87	-15.72
10-Aug-19	-15.21	-13.96	-16.10	-15.59
22-Aug-19	-15.32	-14.88	-16.05	-17.47
3-Sep-19	-16.28	-15.13	-14.20	-15.87
15-Sep-19	-15.98	-15.50	-14.38	-14.14
27-Sep-19	-13.14	-13.93	-13.39	-12.66
9-Oct-19	-15.67	-13.57	-14.51	-12.63
21-Oct-19	-13.70	-12.52	-13.29	-13.78
2-Nov-19	-17.37	-13.92	-13.97	-12.57
14-Nov-19	-18.93	-17.84	-13.24	-13.45
26-Nov-19	-19.34	-16.89	-15.00	-13.92

The detailed analysis of temporal backscattering curve in VH polarization of maize crop showed minimum dB values of

-21.83 to -20.37 during emergence stage and the increased backscatter values at later dates indicating the growth of the crop (-13.98 to -15.14 dB). The backscatter values slightly decreased during the tasseling stage of the maize crop (-16.28 to -15.13 dB) due to decrease in the backscatter values attributing to the sensitivity of radar signal to the tasseling at C-band. The variation in the dB values from seedling to peak vegetative stage was primarily influenced by LAI and biomass of the crop. The backscattering values increased further due to volume scattering and reached a maximum of -13.70 to -12.52 dB at reproductive stages followed by decline in backscattering values due to decrease in greenness and moisture content in leaves of maize crop. The decrease in backscatter values at the later stages might have been probably caused by maturity of the crop, which lowered the water content of the vegetation (Lillesand and Kiefer, 1994) or related to the vegetation biomass and or related to the reduced volumetric scattering due to maturity (Panigrahy and Mishra, 2013). There was mixture of signatures of maize and cotton crops for the images acquired during 15th and 27th Sep. In general maize crop recorded backscattering values -22.82 to -12.52 under VH polarization during its growth phase which is in agreement with the study by Ashmitha et al. (2019), where in backscattering values of maize crop during maturity ranged from -19.04 dB to -14.753 dB for VH polarization.

The crop discrimination with the SAR data is quite challenging as most of the crop growth stages shows similar backscatter coefficients during the initial phase of the crop growth. In case of maize and cotton crops, temporal backscatter showed overlapping response from June to October but precise crop discrimination is feasible in November as maize crop is harvested earlier than cotton crop due to short duration. During this period maize and cotton had the highest separability for discrimination.

3.2. Temporal variables extracted from optical data

Maximum value composites of NDVI images were generated from Sentinel-2 data to minimize the cloud effect in the image. Depending on the availability of the cloud free scenes, some composites were made at fortnightly interval (1FN of June and 1FN of Nov), while, some were made at monthly interval. Among the NDVI images thus derived, first FN of June and July correspond to the sowing period, August, September and October correspond to the crop growth period, while, first FN of November corresponding to the harvesting period of the maize crop. Temporal NDVI profiles constructed from first FN of June to first FN of November images for maize and cotton classes are shown in Figure 3. The profiles showed considerable increase in NDVI from crop emergence to peak vegetative stage (>0.7) and gradual decrease (<0.6) was observed during maturity to harvesting period of the maize crop from October to first FN of November whereas -during the above period these values remain high for cotton crop (Table 3). The NDVI values of maize increased from initial seedling stage to maximum vegetative growth stage with the highest value of 0.75 occurring during August month and then

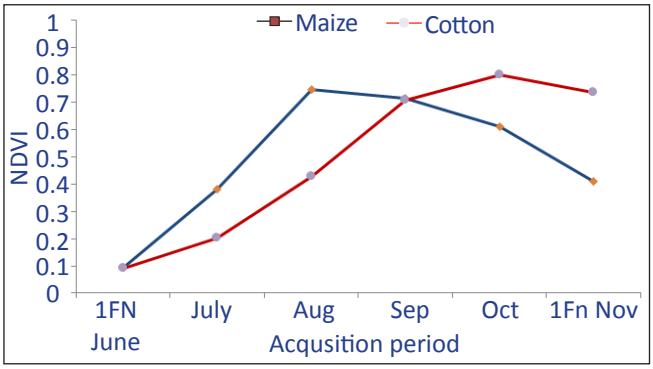

Figure 3: Backscatter intensity values of Temporal VH band (15 layers) for maize and cotton crops

Table 3: Temporal NDVI values of maize and cotton crops

Acquisition period	NDVI values			
	Maize		Cotton	
1FN June	0.08	0.09	0.09	0.08
July	0.23	0.38	0.20	0.17
Aug	0.75	0.74	0.42	0.33
Sep	0.70	0.71	0.70	0.57
Oct	0.60	0.61	0.80	0.72
1FN Nov	0.33	0.40	0.73	0.70

decreasing pattern was observed from maturity to harvesting period. Theoretically, at the early growing stage, the growth rate of healthy vegetation was related to the NDVI, was low due to the limited photosynthesis process caused by many factors such as temperature and chlorophyll content. Then, the growth rate increased due to the optimal temperature, increasing chlorophyll content and other factors. At the later stage, the growth rate decreased due to the deficiency of nitrogen, water and the change of temperature etc. (Lambers et al., 2008).

The results indicate that the time series of the Backscatter intensities and NDVI values of two crop cover class were obviously different, which has been widely used for discrimination of maize and cotton.

4. Conclusion

The Sentinel-1B VH backscatter values of *kharif* crops ranged from -21.83 dB to -12.52 dB at peak growth stage, later the dB values decreased at maturity. The temporal NDVI profiles derived from optical Sentinel-2 data showed higher values (>0.7) in August for maize and cotton crop, whereas at senescence ie., from October to 1st FN of November the maize crop showed lower NDVI values (<0.5). This helped to discriminate the maize crop from cotton crop in Siddipet district of Telanagana state.

6. Acknowledgement

The authors immensely thank National Remote Sensing

Centre, Hyderabad, India for providing the technical guidance and assisting the student in carrying out this work.

7. References

Anonymous, 2019. Agricultural & Processed Food Products Export Development Authority. Maize (apeda.gov.in). https://apeda.gov.in/apedawebsite/SubHead_Products/Maize.htm. Accessed on 02-06-2021.

Ashmitha, N.M., Mohammed, A.J., Pazhanivelan, S., Kumaraperumal, R., Ganesha Raj, K., 2019. Estimation of cotton and maize crop area in Perambalur district of Tamil Nadu using multi-date sentinel-1A SAR Data. International Archives of the Photogrammetry, Remote Sensing and Spatial Information Sciences 42(3), 67–71. DOI:10.5194/isprs-archives-XLII-3-W6-67-2019.

Blaes, X., Vanhalle, L., Defourny, P., 2005. Efficiency of crop identification based on optical and SAR image time series. Remote sensing of environment 96(3-4), 352–365.

Changan, L.I.U., Zhong-xin, C.,Yun, S., Jin-song, C., TuyaHasi., Hai-zhu, P., 2019. Research advances of SAR remote sensing for agriculture applications: A review. Journal of Integrative Agriculture 18(3), 506–525.

Dave,R., Haldar, D., Manjunath, K., Vave, V., Chkraborty, M., Vyas, P., 2019. Identification of cotton crop in Gujarat using multi date RISAT-1 SAR data. Journal of Agrometeorology 21 (Special issue -"NASA 2014" part-III), 1–6.

Ghali, A.A., Wang, K., Shahtahamssebi, A., Xingyu, X., Belete, M., Adam, J.A.G., Kamal, A.M.S., Gan, M., 2020. Mapping maize fields by using multi-temporal sentinel-1a and sentinel-2a images in makarfi, Northern Nigeria, Africa. Sustainability 12, 2539.

Gómez-Chova, L., Tuia, D., Moser, G., Camps-Valls, G., 2015. Multimodal classification of remote sensing images: A review and future directions. Proceedings of the IEEE 103(9), 1560–1584.

Singh, J., Partap, R., Singh, A., Kumar, N., Krity, 2021. Effect of nitrogen and zinc on growth and yield of maize (*Zea mays* L.). International Journal of Bio-resource and Stress Management 12(3), 179–185. DOI: HTTPS://DOI.ORG/10.23910/1.2021.2212.

Lambers, H., Chapin III, F.S., Pons, T.L., 2008. Plant physiological ecology Second Edition. Springer Science and Business Media, 600, ISBN: 978-0-387-78340-6 e-ISBN: 978-0-387-78341-3 DOI: 10.1007/978-0-387-78341-3.

Lillesand, T.M., Kiefer, R.W., 1994. Remote sensing and image interpretation. John Wiley & Sons Inc. New York. ISBN 0471 305 758 https://doi.org/10.1002/gj.3350300217.

Macelloni, G., Paloscia, S., Pampaloni, P., Marliani, F., Gai, M., 2001. The relationship between the backscattering coefficient and the biomass of narrow and broad leaf crops. IEEE Transactions on Geoscience and Remote Sensing 39(4), 873–884.

McNairn, H., Champagne, C., Shang, J., Holmstrom, D., Reichert, G., 2009. Integration of optical and synthetic Aperture Radar (SAR) imagery for delivering operational annual crop inventories. Journal of Photogrammetry and Remote Sensing 64(5), 434–449.

McNairn, H., Ellis, J., Van Der Sanden, J.J., Hirose, T., Brown, R.J., 2002. Providing crop information using RADARSAT-1 and satellite optical imagery. International Journal of Remote Sensing 23(5), 851–870.

Murdia, L.K.1., Wadhwani, R., Wadhawan, N., Bajpai, P., Shekhawat, S., 2016. Maize utilization in India: An overview. American Journal of Food and Nutrition 4(6), 169–176.

Panigrahi, R.K., Mishra, A.K., 2013. Unsupervised classification of scattering behaviour using hybrid-polarimetry. IET Radar, Sonar and Navigation 7(3), 270–276.

Ram, R.L., Sharma, P.K., Chatterjee, T., Kumar, S., Ahmed, N., 2014. Soil resource mapping and assessment of soils at different physiographic divisions in selected mandals of Prakasam district, Andhra Pradesh: A remote sensing and GIS Approach. International Journal of Bio-resource and Stress Management 5(3), 340–349. DOI: 10.5958/0976-4038.2014.00578.8

Shang, J., Champagne, C., McNairn, H., 2006. Agriculture land use mapping using multi-sensor and multi-temporal earth observation data. In Proceedings of the MAPPS/ASPRS 2006 Fall Specialty conference, San Antonio, Texas November 6-10, 2006.

Snehalata, C., Patil, N., Gajanan, S., Meshram, M.R., 2021. A Spatio-temporal study of land use land cover change detection using GIS and remote sensing techniques. International Journal of Bio-resource and Stress Management 12, 026–031. DOI: HTTPS://DOI.ORG/10.23910/1.2021.2138b

Waldhoff, G., Curdt, C., Hoffmeister, D., Bareth, G., 2012. Analysis of multitemporal and multisensor remote sensing data for crop rotation mapping. ISPRS Annals of Photogrammetry, Remote Sensing and Spatial Information Sciences 1–7, 177–182.

Zhou, T., Pan, J., Zhang, P., Wei, S., Han, T., 2017. Mapping winter wheat with multi-temporal SAR and optical images in an urban agricultural region. Sensors 17, 1210.